La-based Perovskite Structures as Efficient Heterogeneous Catalysts for Acceptorless Dehydrogenative Coupling of Alcohols and Amidines toward Pyrimidines

Sándor Balázs Nagy,[‡‖] Anna Adél Ádám,[‡‖] Bence Kutus,[‡] Gergely Ferenc Samu,[‡⁜] Ákos Kukovecz,[†] Zoltán Kónya,[†§] and Gábor Varga*[†]

‡ Department of Molecular and Analytical Chemistry, University of Szeged, Dóm square 7–8, Szeged, H-6721 Hungary
⁜ ELI ALPS, ELI-HU Non-Profit Ltd., Wolfgang Sandner street 3., Szeged, H-6728 Hungary
† Department of Applied and Environmental Chemistry and Interdisciplinary Excellence Centre, University of Szeged, Rerrich Béla tér 1, Szeged, H-6720, Hungary
§ HUN-REN-SZTE Reaction Kinetics and Surface Chemistry Research Group, Rerrich Béla tér 1, H-6720 Szeged, Hungary

*Corresponding author: G. Varga (gabor.varga5@chem.u-szeged.hu)

S1. EXPERIMENTAL PART

S1.1. Materials

All the AR-grade chemical reagents were purchased from Sigma-Aldrich and used as received without further purification.

S1.2. Catalyst preparation

The perovskites ($LaNiO_3$, $LaMnO_3$, $LaCoO_3$) were prepared by the well-known citric acid process with little modifications. Briefly, $La(NO_3)_3 \times 6H_2O$ and $Mn(NO_3)_2 \times 6H_2O$ or $Co(NO_3)_2 \times 6H_2O$ or $Ni(NO_3)_2 \times 6H_2O$ aqueous solutions were made by dissolving the salts in deionized water with citric acid respecting the 1:1:2.4 molar ratio (La^{3+} : M(II) : citric acid). The pH was set between 8–9 with 10% ammonium hydroxide solution. The mixture was evaporated on a hot plate to form a gel, dried at 130 ºC overnight, calcined 300 ºC for 5 h and after grinding, sintered at 850 ºC for 24 h.[1]

The Ruddlesden-Popper (RP) phase layered perovskite materials were prepared based on modified sol-gel methods. For the synthesis of $La_{n+1}Mn_nO_{3n+1}$ compounds two mother liquors (solution A and B) were made. While Solution A contained appropriate amount of metal salts ($La(NO_3)_3 \times 6H_2O$, $Mn(NO_3)_2 \times 6H_2O$ and $MnCl_2 \times 4H_2O$), citric acid and 10% ammonium hydroxide were added to deionized water for solution B and then the solutions were mixed up with each other. Solution A and B were mixed and evaporated slowly on a hotplate to form a gel. The obtained gel was dried at 130 ºC overnight, combusted at 700 ºC for 5 hours, grinded then pelleted at 5 tons pressure then sintered at 1000 ºC for 12 hours with a temperature ramp rate of 10 ºC/min. After cooling the sintered pellet was grinded, pelleted and sintered again at 1000 ºC for 12 hours with the same temperature ramp.[2]

The layered $La_{n+1}Co_nO_{3n+1}$ and $La_{n+1}Ni_nO_{3n+1}$ compounds were synthesized by a standard combined ethylenediaminetetraacetic acid (EDTA)–citrate complexing sol gel process. Stoichiometric amounts of the metal nitrate salts were dissolved in deionized water in a glass beaker and stirred by using a magnetic stir bar. Then, EDTA and citric acid were added to the solution as complexing agents with molar ratio of EDTA/total metal ions/citric acid maintained as 1:1:2. The solution pH was adjusted to 7 by adding 10% aqueous solution of NH_3. The obtained solution was evaporated slowly to form a gel. The gel was dried at 175 ºC overnight, combusted at 450 ºC for 5 hours, pelleted and sintered at 1100 ºC for 110 hours with two intermediate grinding (24+48+38 hours) and pelleting step.[3]

S1.3. Catalyst characterization

Powder X-ray diffraction (XRD) was performed with a Rigaku Miniflex II instrument applying CuKα radiation (λ = 0.15418 nm) and 40 kV accelerating voltage at 30 mA. he characteristic reflections were identified based on the database JCPDS-ICDD (Joint Committee of Powder Diffraction Standards- International Centre for Diffraction Data). Crystallite sizes were determined by Scherrer equation:

$$D = \frac{K\lambda}{\beta\cos\theta} \quad (1)$$

where K is the Scherrer constant, λ is wave length of the X-ray beam used, β is the full width at half maximum (FWHM) of the peak and θ is the Bragg angle.

The morphology of the structures was studied by Transmission Electron Microscopy (TEM – FEI TECNAI G220 X-Twin) operated at voltage of 200 kV. The samples were dispersed in ethanol and drop-cast onto carbon film-coated copper grids. The acidity of the samples was mapped by a BELCAT-A catalyst analyzer equipped with a thermal conductivity detector (TCD). Before the measurements, the solids were degassed in helium flow at 300 ºC for 60 min to ensure clean surface. The NH_3–temperature-programmed desorption (NH_3–TPD) curves were registered after the saturation step at 90 ºC than the solids were heated with a temperature ramp rate of 10 º/min up to 600 ºC.

For determining the surface area of the as-prepared samples, BET (Brunauer-Emmett-Teller) N_2-sorption experiments were performed, using a NOVA3000 (Quantachrome) instrument. Prior to the measurements, the solids were degassed with N_2 at 100 °C for 5 hours under vacuum to clean the surface from the adsorbents. The measurements were carried out at the temperature of liquid N_2. The actual La-to-M(III) ratios (M: Mn, Co, Ni) of the samples were detected with an Agilent 7900 ICP-MS (inductively coupled plasma–mass spectrometry) (Agilent Technologies) device. ICP multielement standard solution IV (CertiPUR) was used for the quantitative analysis. Before the measurements, an accurately measured amount (a few milligrams) of the solids was dissolved in 5 mL of cc. HNO_3. After dissolution, the samples were diluted to 100 mL with distilled water and filtered.

X-ray photoelectron spectra (XPS) were taken by a SPECS instrument equipped with a PHOIBOS 150 MCD 9 hemispherical analyzer, under a main-chamber pressure in the 10^{-9}–10^{-10} mbar range. The analyzer was used in a fixed analyzer transmission (FAT) mode with 20 eV pass energy. The Al Kα radiation (hν = 1486.6 eV) of a dual anode X-ray gun was the excitation source. The gun was run at 210 W power (14 kV, 15 mA). The binding energy scale was set by considering the position of the main C 1 s component to 285.0 eV in all cases. For

evaluating the obtained data, commercial (CasaXPS, Origin) software packages were applied. Dynamic light scattering (DLS) was used to measure the solvodynamic size of the aggregated perovskite particles in 2-Me-THF. The measurements were carried out with a Nanosizer (Malvern) device as above at 175° scattering angle in disposable plastic cuvettes (VWR).

4.4. Optimized procedure for the three-component catalytic acceptorless dehydrogenative coupling (ADC) reactions for pyrimidine synthesis from primary and secondary alcohols and benzamidines

In an optimized reaction sequence (Scheme 1), first a 10 mL one-neck round bottom flask was charged with the catalyst (5 mol % with the respect to benzamidine × HCl), benzamidine × HCl (0.75 mmol) and potassium tert-butoxide (^{t}BuOK) (1.5 equiv., 1.125 mmol) which were dissolved in 2-Methyltetrahydrofuran (2-MeTHF) of 2 mL, then secondary alcohol (0.75 mmol), primary alcohol (0.75 mmol) and a magnetic stir bar were added to the mixture. The flask was refluxed and magnetically stirred (600 rpm) for 8 hours. After the reaction, the catalyst was removed by a MiniStar Silver microcentrifuge (VWR) at 6000 rpm. The obtained crude product was analyzed after the necessary dilution with 2-Me-THF. For the solvent screening and other reaction optimizations, kinetic studies, and control reactions, the conversion of benzyl alcohol and yield of products were determined by using GC-MS. For quantification, internal standard method was introduced during the GC-MS measurements for which n-tetradecane was used as an internal standard. The reactants and products of the reactions were analyzed by gas chromatography (Agilent 8890) equipped with a HP-5 column (30 m × 0.25 mm × 0.25 μm) and mass (MS) detector, in which the carrier gas was helium. The commercially available products were identified by using authentic samples. The identification of the commercially non-available products occurred by combining (GC-)MS, ^{1}H- and ^{13}C-NMR spectroscopies. Data can be found in the “Supporting Information”. A Bruker DRX500 500 MHz NMR spectrometer was used for NMR spectroscopy. All samples were dissolved in the corresponding deuterated organic solvents and NMR spectra were recorded at room temperature. The selectivity (mol%) data were calculated as the quotient of the actual product yield and benzyl alcohol conversion, multiplied by 100%.

The hot filtration experiments were performed as follows. After refluxing the reaction mixture for 2 hours, the catalyst was filtered from the reaction mixture, and the flask was placed back to reflux another 4 hours. Kinetic curve was determined for this hot filtrated sample in comparison to the normal one treated parallel with above-described.

The catalysts reusability was tested as follows. After the reaction, the catalyst was separated from the reaction mixture by centrifugation, washed with the solvent (2 mL), dried at

130 ºC for 1 hour. The dried catalyst was placed back in a round-bottom flask and was refluxed in chloroform (10 mL) for 1 hour to ensure that all of the remaining organic materials were separated from the catalyst. The catalyst structure was re-examined with XRD after each washing step and then the perovskite was reused in a new catalytic run under the same optimized reaction conditions. The leaching of the metal component was monitored by the analysis of the crude products with the aid of ICP-MS technique.

To compare the activity of the catalysts, the turnover frequencies (TOFs) were determined. For this purpose, the TOFs were calculated from the initial stage of the linear regime of the kinetic curves for the corresponding catalytic reactions. The TOFs are given by dividing the initial reaction rates by the number of active cobalt and lanthanum atoms in the perovskite and the reaction time needed.

To decide the existence of a true synergistic effect between lanthana and Co(III) sites, a two-way ANOVA analysis was completed.[4] Briefly, in this statistical probe, the focus is on the response (μ) of three of the treatment groups (A, B, A+B) compared to the fourth (C), control group (i.e. neither treatment A nor B). In our case, the three groups were the catalytic performance of pure La_2O_3 (A), the pure Co_3O_4 (B) and that of their physical mixture or the $LaCoO_3$ (A+B). The comparative fourth (C) was the system in the absence of any catalyst. The obtained yield was chosen as the response (μ). The statistical null hypothesis for this method can be given by:

$$H_0: (\mu_{A+B} - \mu_C) = (\mu_A - \mu_C) + (\mu_B - \mu_C) \quad (2)$$

If this equation is true, the response of the A and B groups were added up and no synergism but there is an additive effect. When the left side higher than the right side, there is a real synergism. Conversely, antagonistic effect must be associated with the trend.

In order to quantify the difference between the commonly used Pt/C and $LaCoO_3$ perovskite from an environmental point of view, the isolated yield and EcoScale (Table S4) were determined for both under the different optimal reaction conditions. For EcoScale scoring, the following scoring system was used:

Parameter	Penalty points
1. Yield	(100 – %yield)/2
2. Price of reaction components (to obtain 10 mmol of end product)	
Inexpensive (< $10)	0
Expensive (> $10 and < $50)	3
Very expensive (> $50)	5
3. Safety	
N (dangerous for environment)	5
T (toxic)	5
F (highly flammable)	5
E (explosive)	10
F+ (extremely flammable)	10
T+ (extremely toxic)	10
4. Technical setup	
Common setup	0
Instruments for controlled addition of chemicals	1
Unconventional activation techniquec	2
Pressure equipment, > 1 atmd	3
Any additional special glassware	1
(Inert) gas atmosphere	1
Glove box	3
5. Temperature/time	
Room temperature, < 1 h	0
Room temperature, < 24 h	1
Heating, < 1 h	2
Heating, > 1 h	3
Cooling to 0°C	4
Cooling, < 0°C	5
6. Workup and purification	
None	0
Cooling to room temperature	0
Adding solvent	0
Simple filtration	0
Removal of solvent with bp < 150°C	0
Crystallization and filtration	1
Removal of solvent with bp > 150°C	2
Solid phase extraction	2
Distillation	3
Sublimation	3
Liquid-liquid extraction	3
Classical chromatography	10

S2. SUPPORTING RESULTS

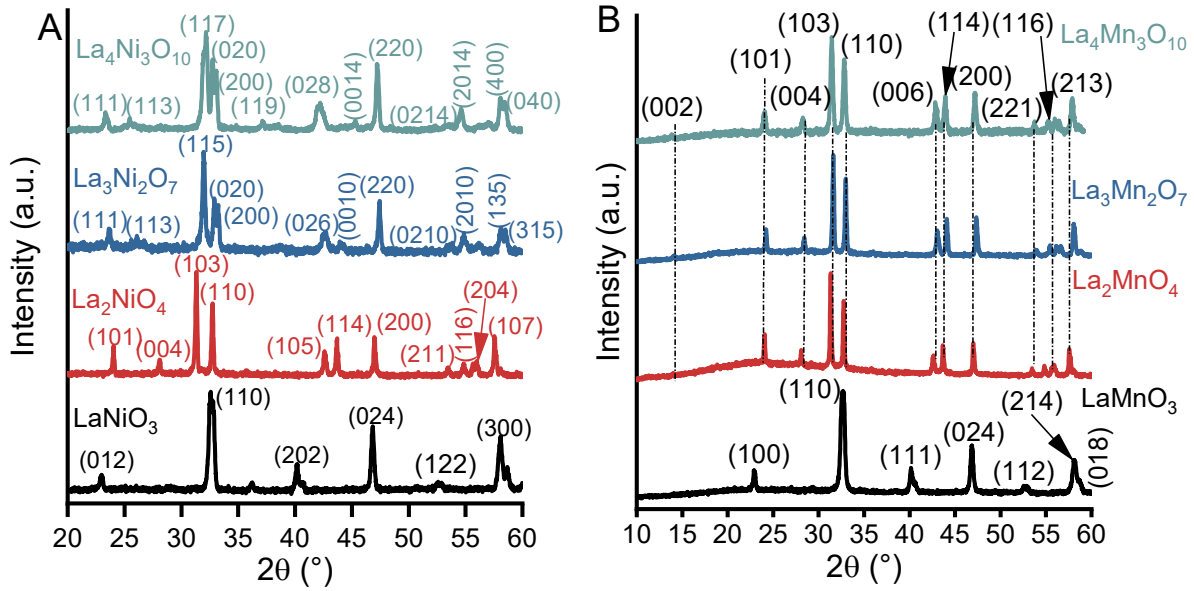

Figure S1. XRD patterns of perovskite and Ruddlesden-Popper phase oxides. (A) Ni-containing lanthana systems (perovskite: PDF#34–1028; La_2Ni–RP-phase: PDF#011–0557; La_3Ni_2–RP-phase: PDF#50–0244; La_4Ni_3–RP-phase: PDF#50–0243) and (B) Mn-containing lanthana systems (perovskite: PDF#01–075-0440, RP-phase: PDF#400002).

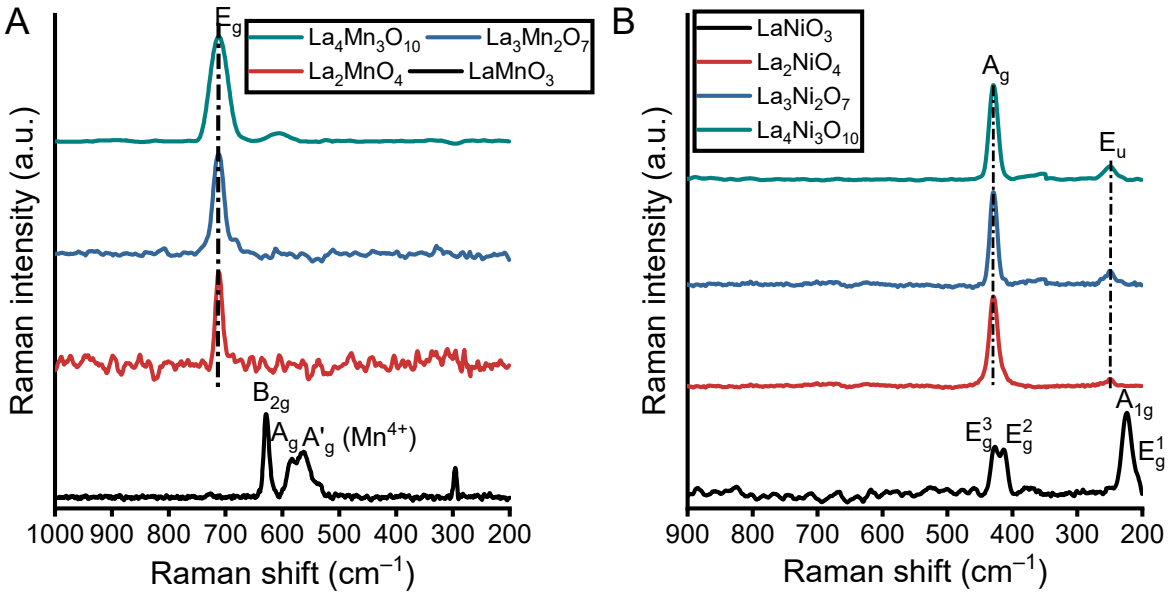

Figure S2. Raman spectra of perovskite and Ruddlesden-Popper phase oxides. (A) Ni-containing lanthana systems and (B) Mn-containing lanthana systems.

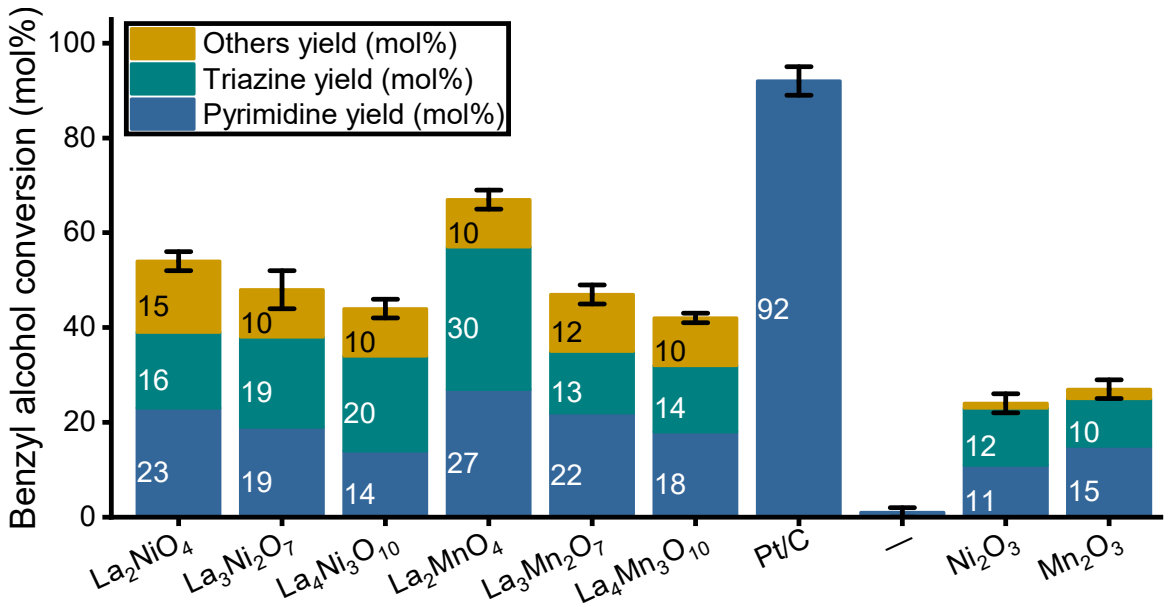

Figure S3. ADC reaction of benzyl alcohol (0.25 mmol), phenyl ethanol (0.25 mmol) and benzamidine hydrochloride (0.25 mmol) in the presence of 2 eq. ^{t}BuOK and 10 mol% of various potential catalysts. Reaction conditions: reflux temperature, toluene of 2 mL, t = 24 h under a N_2 atmosphere.

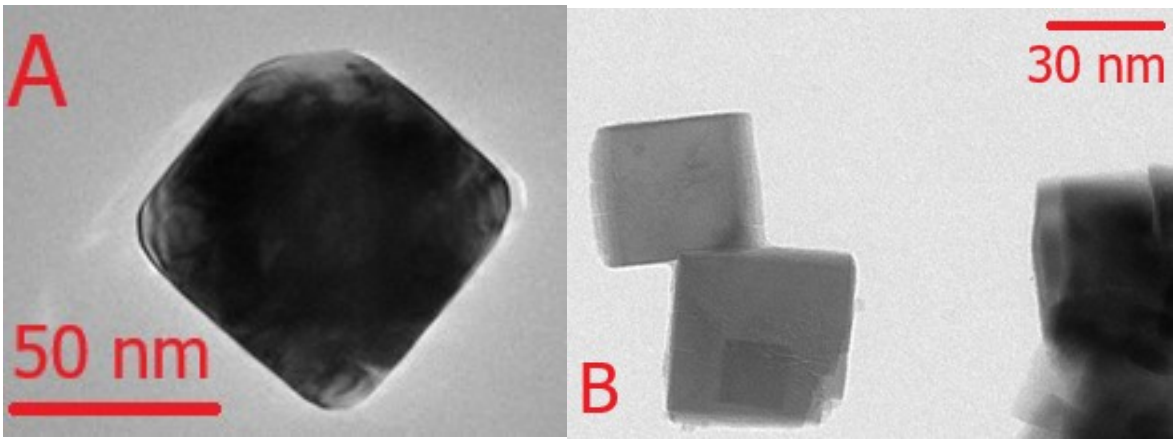

Figure S4. TEM images of $LaCoO_3$ (A) and $LaMnO_3$ (B).

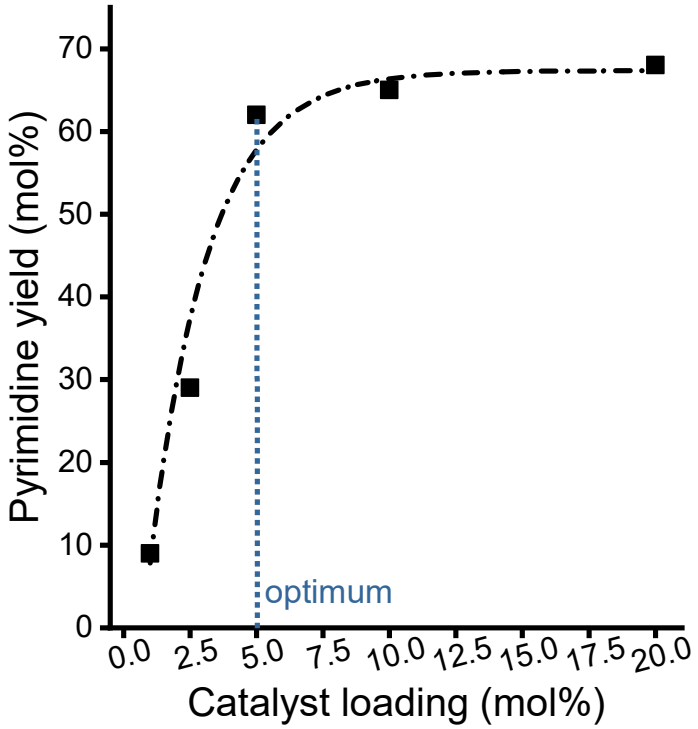

Figure S5. Optimization of the reaction parameters for heterogeneous ADC reaction catalyzed by $LaCoO_3$: effect of the catalyst loading. Reaction conditions: benzyl alcohol (0.25 mmol), phenyl ethanol (0.25 mmol) and benzamidine hydrochloride (0.25 mmol) in the presence of 1.5 eq. ^{t}BuOK and variable loading of $LaCoO_3$, reflux temperature, 2-Me-THF of 2 mL, t = 24 h under an air atmosphere.

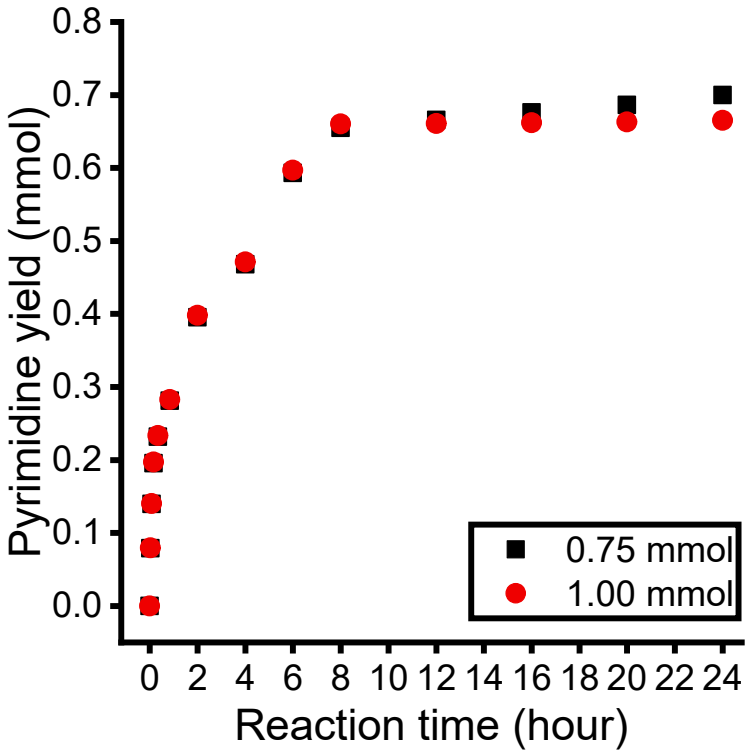

Figure S6. Optimization of the reaction parameters for heterogeneous ADC reaction catalyzed by $LaCoO_3$: parallel optimization of reaction time and reactant concentrations. Reaction conditions: benzyl alcohol (0.75 or 1.00 mmol), phenyl ethanol (0.75 or 1.00 mmol) and benzamidine hydrochloride (0.75 or 1.00 mmol) in the presence of 1.5 eq. ^{t}BuOK and 5mol% of $LaCoO_3$, reflux temperature, 2-Me-THF of 2 mL, t = 24 h under an air atmosphere.

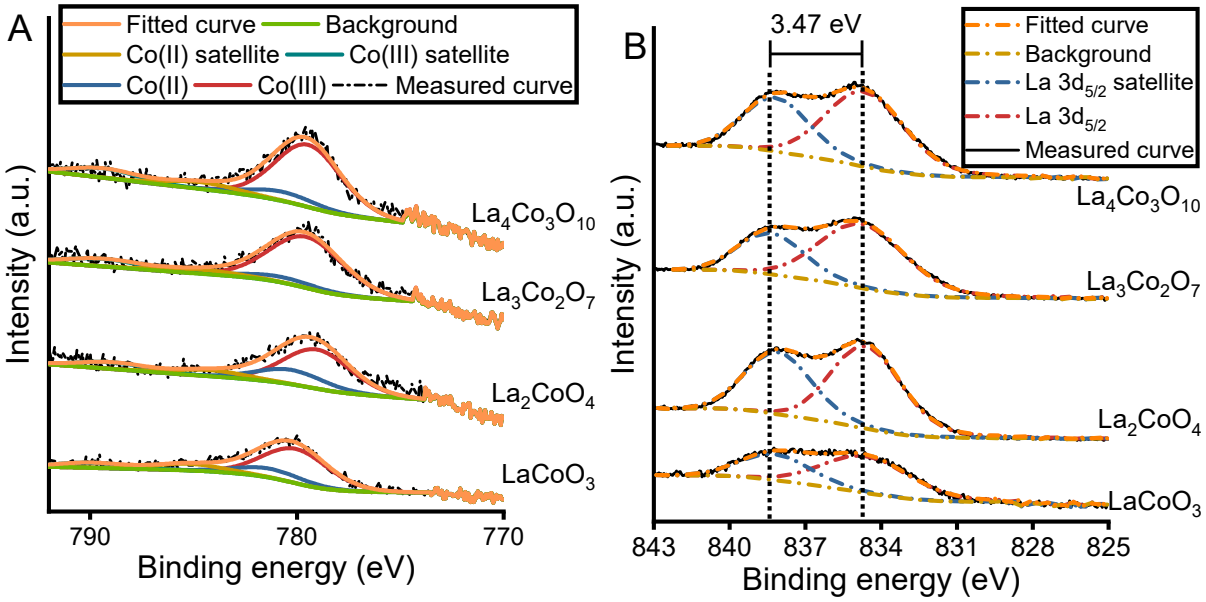

Figure S7. XP spectra of the Co-containing perovskite and RP-phase systems. Co_{2p} (A) and La_{3d} spectra (B).

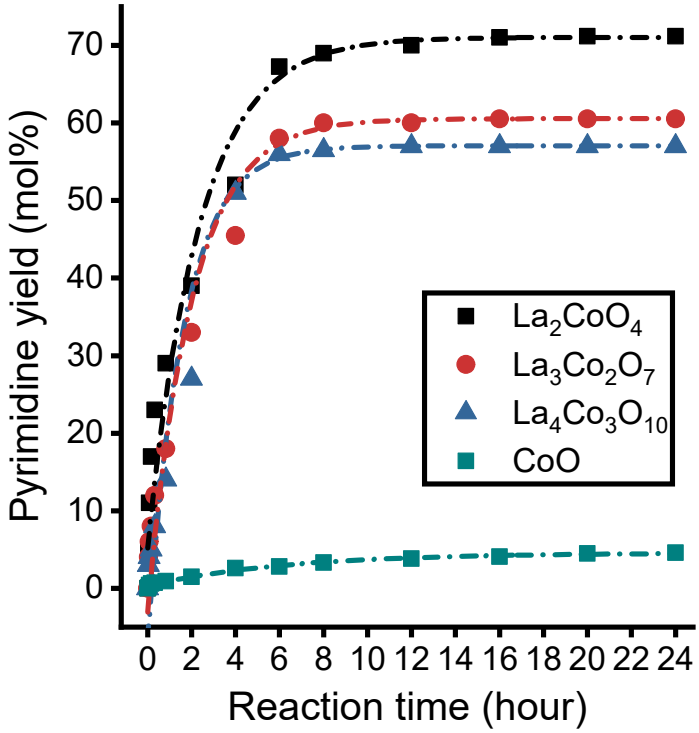

Figure S8. Kinetic curve of the ADC test reactions catalyzed by the as-prepared monometallic and bimetallic La/Co oxide catalysts. Reaction conditions: benzyl alcohol (0.75 mmol), phenyl ethanol (0.75 mmol) and benzamidine hydrochloride (0.75 mmol) in the presence of 1.5 eq. ^{t}BuOK and 5 mol% of various oxide catalysts, reflux temperature, 2-Me-THF of 2 mL, t_{max} = 24 h under an air atmosphere.

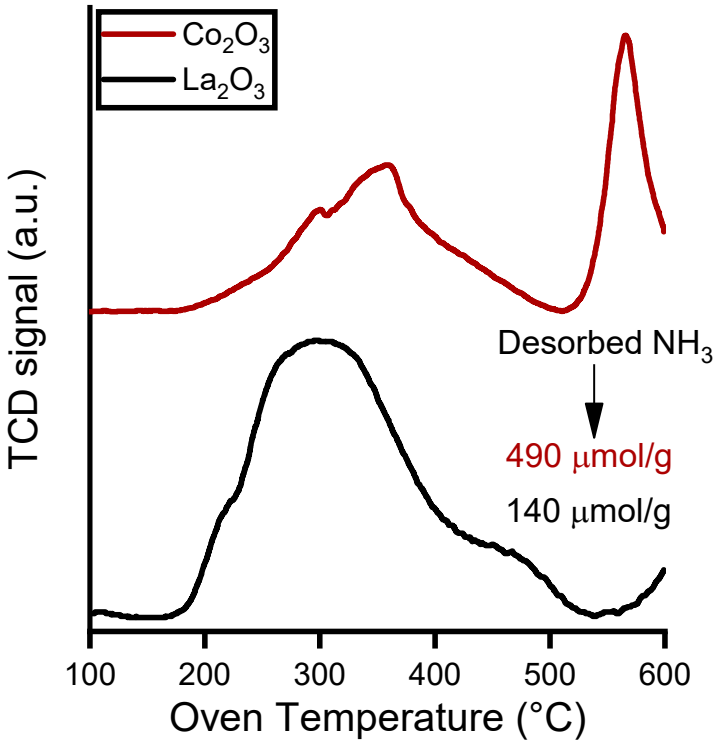

Figure S9. NH_3–TPD profile of La_2O_3 and Co_2O_3.

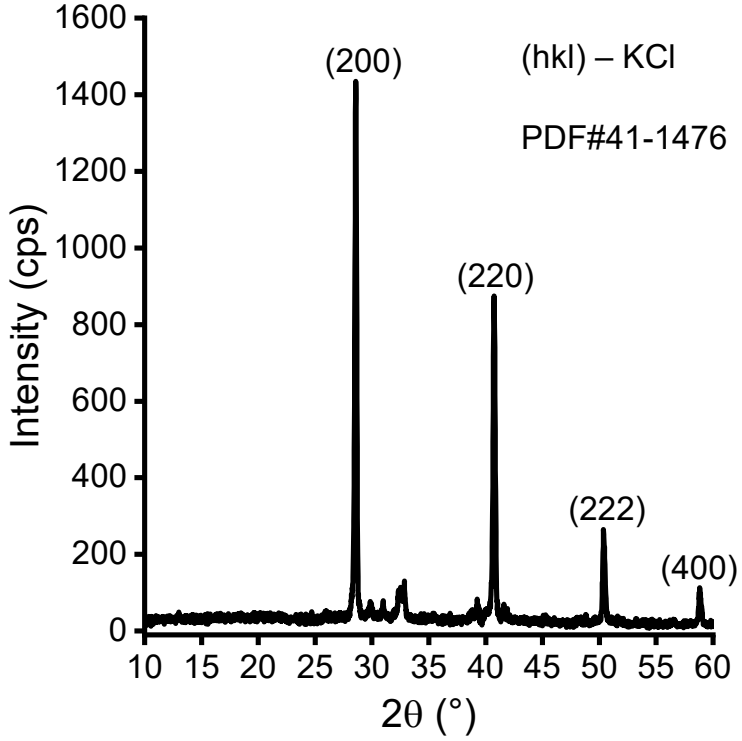

Figure S10. XRD patterns of spent $LaCoO_3$ catalyst after the 11th catalytic cycle.

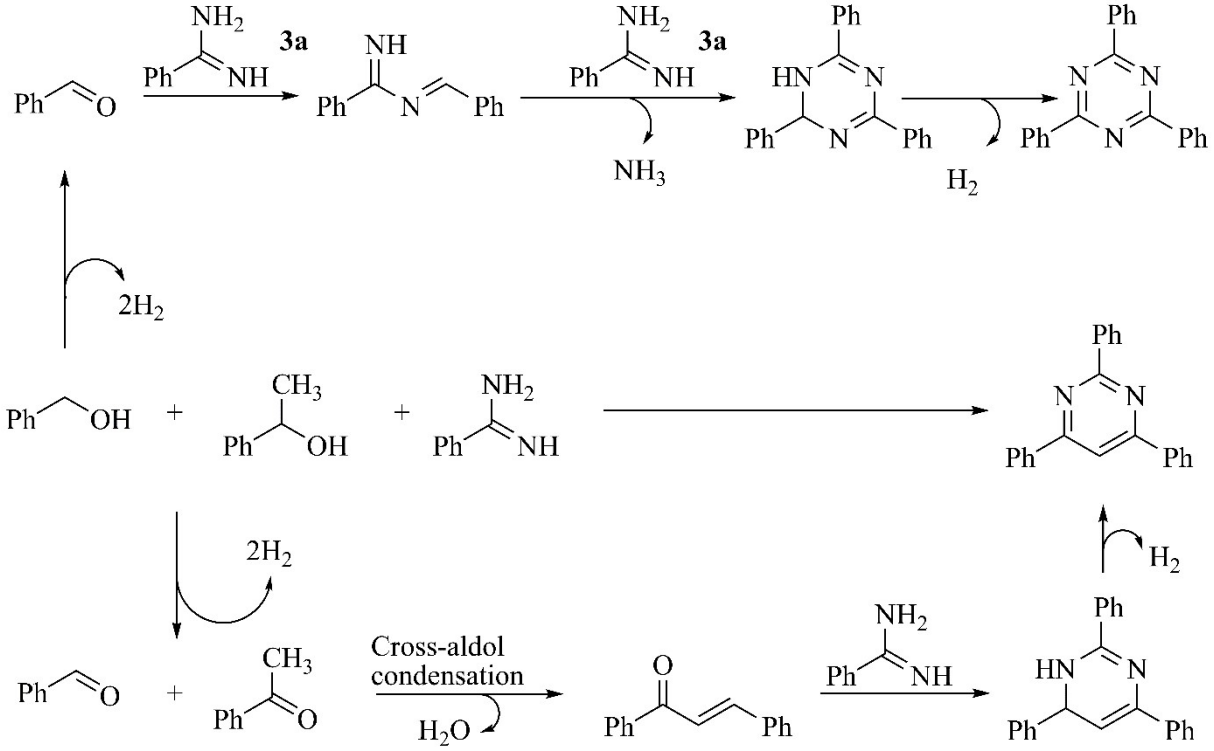

Scheme S1. Classic mechanism of pyrimidine synthesis via a three component ADC reaction from alcohols and benzamidines (lower). Mechanism of the most common side-reaction of these pyrimidine-derivative syntheses providing triazines. Based on Shimizu, Sidiki and their co-workers' study.[5] (In this study Pt/C heterogeneous catalyst was used.)

Table S1. Compositional and textural characteristics of the transition metal oxides tested in three components cyclisation.

	Oxide	La/M[a] ratio	Specific surface area (m^2/g)[b]	Primer crystallite size (nm)[c]
1	La_2O_3	—	39	—
2	Co_3O_4	—	18	—
3	$LaCoO_3$	0.95	40	25
4	La_2CoO_4	1.93	55	40
5	$La_3Co_2O_7$	1.47	49	45
6	$La_4Co_3O_{10}$	1.28	53	43
7	$LaMnO_3$	0.97	21	20
8	La_2MnO_4	1.90	44	39
9	$La_3Mn_2O_7$	1.49	36	41
10	$La_4Mn_3O_{10}$	1.29	41	38
11	$LaNiO_3$	0.97	33	23
12	La_2NiO_4	1.43	29	46
13	$La_3Ni_2O_7$	1.46	46	41
14	$La_4Ni_3O_{10}$	1.35	54	40
15	NiO	—	50	—
16	Mn_2O_3	—	40	—

a: M: Mn, Co, Ni; determined by ICP-MS; b: determined by BET measurements; c: calculated based on the Scherrer equation from the most intense peak of the corresponding XR diffractogram.

Table S2. Optimization procedure of ADC reaction of alcohols and benzamidine toward pyrimidine over $LaCoO_3$ catalyst. Initial reaction conditions: benzyl alcohol (0.25 mmol), phenyl ethanol (0.25 mmol) and benzamidine hydrochloride (0.25 mmol) in the presence of 2 eq. ^{t}BuOK and 10 mol% of $LaCoO_3$, reflux temperature (T = 80 °C), 2-Me-THF of 2 mL, t = 24 h under a N_2 atmosphere.

	Solvent	**Temperature (°C)**	**Reactants ratio[c]**	**Added base**	**Base loading (eq.)[d]**	**Benzaldehyde conversion (mol%)**	**Pyrimidine selectivity (mol%)**	**Pyrimidine yield (mol%)**
1[f]	2-Me-THF[a]	**80**[b]	1:1:1	^{t}BuOK	2	65	100	65
2[f]	2-Me-THF	60	1:1:1	^{t}BuOK	2	30	98	29
3[f]	2-Me-THF	100	1:1:1	^{t}BuOK	2	79	79	62
4[f]	2-Me-THF	120	1:1:1	^{t}BuOK	2	89	54	48
5	2-Me-THF	80	1:1:1	**^{t}BuOK**	2	64	100	64
6	2-Me-THF	80	1:1:1	KOH	2	44	97	43
7	2-Me-THF	80	1:1:1	NaOH	2	41	96	39
8	2-Me-THF	80	1:1:1	Cs_2CO_3	2	30	95	28
9	2-Me-THF	80	1:1:1	K_2CO_3	2	24	96	23
10	2-Me-THF	80	1:1:1	^{t}BuOK[e]	2	45	97	44
11	2-Me-THF	80	1:1:1	KOH[e]	2	45	94	42
12	2-Me-THF	80	1:1:1	NaOH[e]	2	41	95	39
13	2-Me-THF	80	1:1:1	Cs_2CO_3[e]	2	54	97	52
14	2-Me-THF	80	1:1:1	K_2CO_3[e]	2	45	100	45
15	2-Me-THF	80	1:1:1	^{t}BuOK	**1.5**	63	100	63
16	2-Me-THF	80	1:1:1	^{t}BuOK	1	47	80	38
17	2-Me-THF	80	1:1:1	^{t}BuOK	0.5	20	61	12
18	2-Me-THF	80	1:1:0.5	^{t}BuOK	2	44	99	86
19	2-Me-THF	80	1:0.75:0.5	^{t}BuOK	2	39	100	78
20	2-Me-THF	80	0.5:0.5:1	^{t}BuOK	2	76	77	29
21	2-Me-THF	80	0.5:0.75:1	^{t}BuOK	2	100	70	35
22	**2-Me-THF**	**80**	**1:1:1**	**^{t}BuOK**	**2**	**63**	**100**	**63**

a: 2-Me-THF: 2-methyltetrahydrofuran; b: reflux temperature in 2-Me-THF; c: Benzyl alcohol : phenyl ethanol : benzamidine hydrochloride; d: eq. = equivalent to the amount of benzyl alcohol; e: in an 1:1 solvent mixture of 2-Me-THF and ethanol; f: under a nitrogen atmosphere (further experiments (from entry 5) were carried out under an air atmosphere). The measures in bold were selected as optimal conditions.

Table S3. Solvodynamic diameter of the perovskite oxide aggregates in 2-Me-THF.

Perovskite	**Solvodynamic diameter (nm)**
$LaCoO_3$	811
$LaMnO_3$	878
$LaNiO_3$	820

Table S4. Listed catalytic performance of the well-recognized benchmark catalyst for one-pot, three component synthesis of pyrimidines from alcohols and benzamidines in comparison to that of our as-prepared $LaCoO_3$ catalyst.

	Catalyst	Pyrimidine yield (mol%)	Pyrimidine selectivity (mol%)	Solvent	Base loading (eq.)	Reaction time (h)	Reaction temperature (°C)	Reusable (cycles)	Atmos -phere	Refs.
1	***$LaCoO_3$***	*87*	*100*	*2-Me-THF*	*1.5*	*8*	*80*	*8 + 2 (after regeneration)*	*air*	***This work***
2	**Pt/C**	92	100	toluene	1.2 eq.	24	110	5	N_2	5
3	**Ni(II)-pincer complex**	84	95	toluene	0.5 eq.	24	110	No	N_2	6
4	**Mn-pincer complex***	92	100	1.4-dioxane	1.1	20	120	No	N_2	7
5	**Ir-pincer complex***	83	100	tert-Amyl alcohol	0.7	24	105	No	N_2	8
6	**Re(I)-pincer complex***	84	100	toluene	0.75	8	140	No	N_2	9
7	**Mn(I)-pincer complex***	86	100	toluene	1.5	24	140	No	N_2	10

*In these works, alcohol-excess was used to complete the reaction.

Table S5. Comparison of the recyclable catalysts (Pt/C, $LaCoO_3$) for pyrimidine synthesis via a three component ADC reaction based on EcoScale.

	Pt/C[5]	**$LaCoO_3$ (this work)**
Yield	6 (88 mol%)**	8 (84 mol%)**
Price of reaction components	3 (expensive)[a]	0
Safety	10 (toluene: flammable and toxic)[b]	5
Technical setup	4 (special glassware, inert atmosphere, pressure equipment for Pt/C activation)	0
Temperature/time	3 (heating 24h)	3(heating 8h)
Workup and purification	10 (classical chromatography)	3 (distillation)
Overall	36	19
Ecoscale[11]	**64**	**81***

*A higher a value means greener process. Over Ecoscale of 80, systems can be regarded as green process. **Isolated yields.[6] a: (> $10 and < $50). b: Based on the hazard warning symbols. C:

Table S6. NH_3-TPD and BET measurements of the as-prepared and spent catalyst after the 8th cycle.

Catalyst	NH_3 adsorbed (µmol/g)	Specific surface area (m^2/g)[a]	Acidic site density (µmol/m^2)[b]
As-prepared	205	40	5.125
Spent	110	33	3.333

a: calculated from BET data. b: NH_3 adsorbed/Specific surface area

Table S7. Synthesis of pyrimidines from different primary alcohols. Reaction parameters: primary alcohol (0.75 mmol), secondary alcohol (0.75 mmol) and amidine (0.75 mmol) in the presence of 1.5 eq. ^{t}BuOK and 5 mol% of $LaCoO_3$, reflux temperature, 2-Me-THF of 2 mL, t = 12 h under aerobic conditions.

Reactants	Conversion (mol%)	Selectivity (mol%)
2-phenylethanol	92	100
2-phenoxyethanol	85	95
3-phenylpropanol	87	96

S3. SPECTRAL AND CHROMATOGRAPHIC DATA OF THE COMMERCIALLY NON-AVAILABLE, AS-SYNTHESIZED PYRIMIDINE DERIVATIVES

4-methyl-2,6-diphenylpyrimidine

^{1}H NMR (500 MHz, $CDCl_3$, TMS): δ 8.59 (d, J = 7.5 Hz, 2 H), 8.29–8.18 (m, 2 H), 7.58–7.44 (m, 7 H), 2.66 (s, 3 H).

^{13}C NMR (125 MHz, $CDCl_3$, TMS) δ 24.6, 114.0, 127.1, 128.3, 128.4, 128.8, 130.4, 130.6, 137.2, 138.1, 163.6, 164.2, 167.7.

MS (EI, 70 eV) m/z: 246.2 ($M^{+\cdot}$), 143.1, 102.1, 77.1.

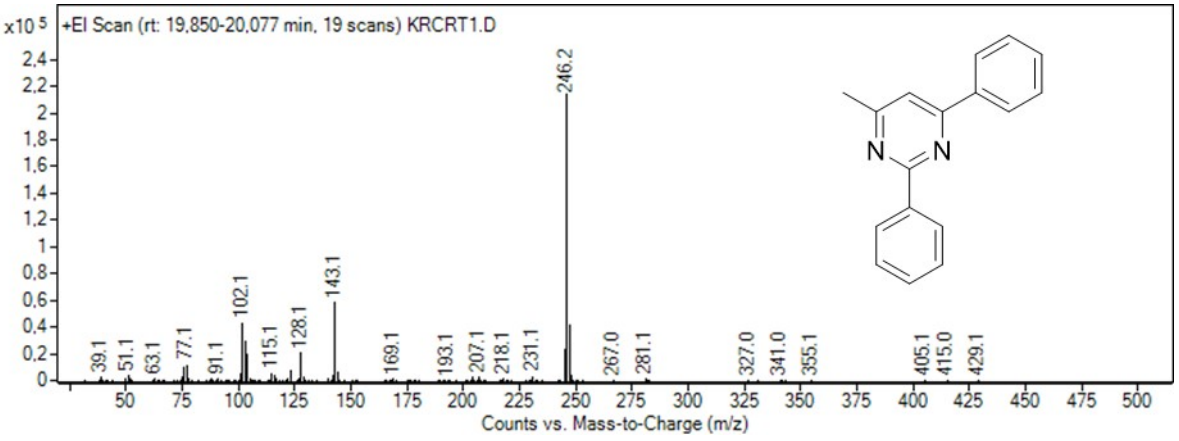

*4-ethyl-2,6-diphenylpyrimidine (**4b**)*

^{1}H NMR (500 MHz, $CDCl_3$, TMS): δ 8.62 (d, *J* = 6.6 Hz, 2H), 8.23 (d, *J* = 7.0 Hz, 2H), 7.55-7.47 (m, 7H), 2.93 (q, 2H), 1.44 (t, 3H).

^{13}C NMR (125 MHz, $CDCl_3$): δ 172.7, 164.4, 138.4, 137.9, 130.9, 130.7, 130.2, 129.2, 128.9, 128.7, 127.4, 112.9, 31.4, 13.0.

MS (EI, 70 eV) m/z: 259.2, 260.2 ($M^{+\cdot}$), 261.2, 232.1, 156.1, 129.1, 115.1, 104.1, 77.1.

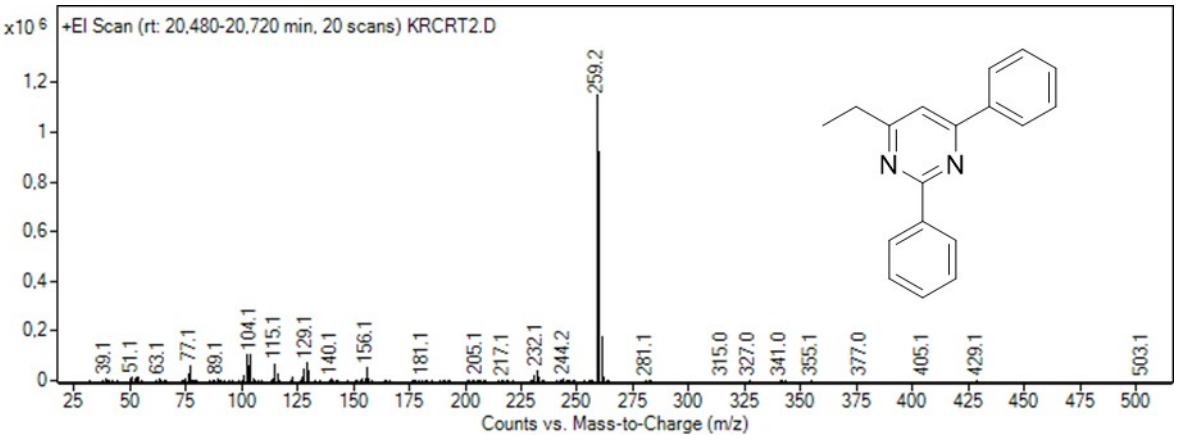

4-isobutyl-2,6-diphenylpyrimidine

^{1}H NMR (500 MHz, $CDCl_3$, TMS): δ 8.74 (d, *J* = 7.27 Hz, 2H), 8.30 (d, *J* = 7.08 Hz, 2H), 8.03 (s, 1H), 7.63-7.46 (m, 7H), 4.23 (m, 1H), 1.03 (d, J = 6.6 Hz, 3H).

^{13}C NMR (101 MHz, $CDCl_3$): δ 170.2, 164.3, 156.7, 138.0, 130.5, 128.5, 128.2, 118.8, 47.1, 28.4, 22.5.

MS (EI, 70 eV) m/z: 288.2 ($M^{+\cdot}$), 273.2, 246.2, 143.1, 128.1, 115.1, 104.1, 77.1.

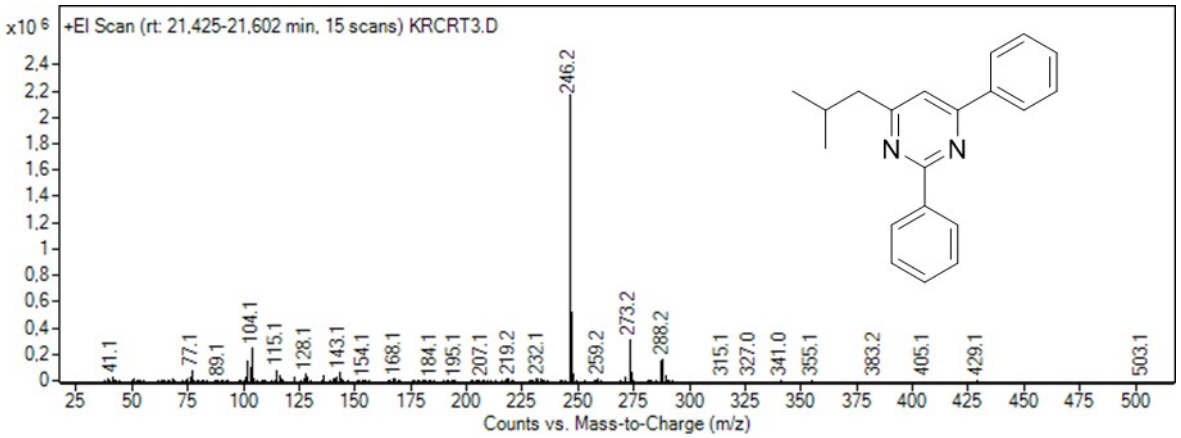

4-butyl-2,6-diphenylpyrimidine

^{1}H NMR (500 MHz, $CDCl_3$, TMS): δ 8.63 (dd, *J* = 7.95 Hz, 2H), 8.23 (m, 2H), 7.65-7.2 (m, 7H), 2.9 (t, 2H), 1.86 (m, 2H), 1.5 (dd, *J* = 10.52 Hz, 2H), 1.01 (t, *J* = 7.38 Hz, 3H).

^{13}C NMR (101 MHz, $CDCl_3$): δ 170.2, 164.3, 156.7, 138.0, 130.5, 128.5, 128.2, 118.8, 47.1, 28.4, 22.5.

MS (EI, 70 eV) m/z: 288.2 ($M^{+\cdot}$), 273.2, 259.2, 246.2, 143.1, 128.1, 115.1, 104.1, 77.1.

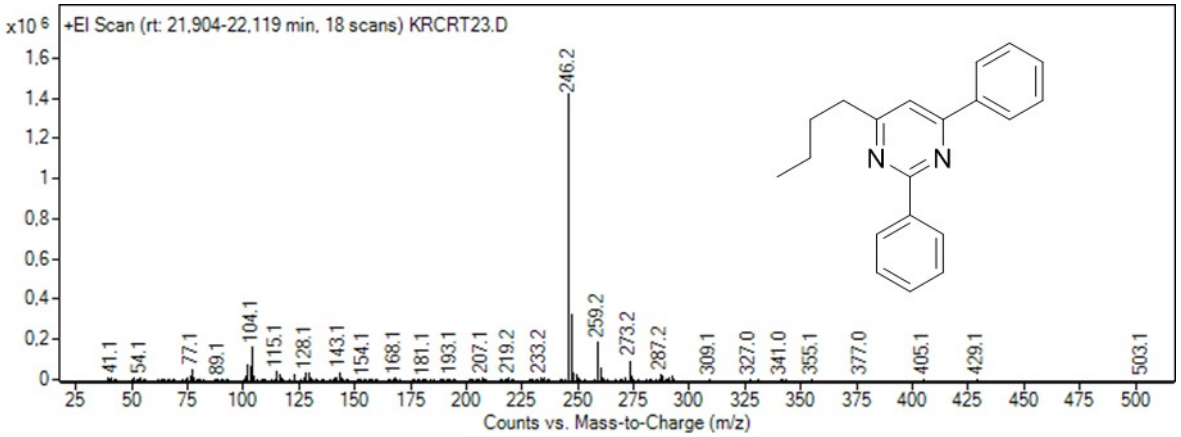

4-hexyl-2,6-diphenylpyrimidine

^{1}H NMR (500 MHz, $CDCl_3$, TMS): δ 8.61 (m, 2H), 8.18 (m, 2H), 7.5-7.4 (m, 6H), 7.38 (s, 1H), 2.83 (m, 2H), 1.83 (m, 2H), 1.4-1.3 (m, 6H), 0.89 (m, 3H).

^{13}C NMR (101 MHz, $CDCl_3$): δ 171.1, 164.3, 156.8, 138.0, 130.4, 128.5, 128.2, 117.9, 38.0, 31.9, 29.3, 28.7, 22.7, 14.12.

MS (EI, 70 eV) m/z: 316.2 ($M^{+\cdot}$), 301.2, 287.2, 273.2, 259.2, 246.2, 193.1, 143.1, 128.1, 115.1, 104.1, 77.1.

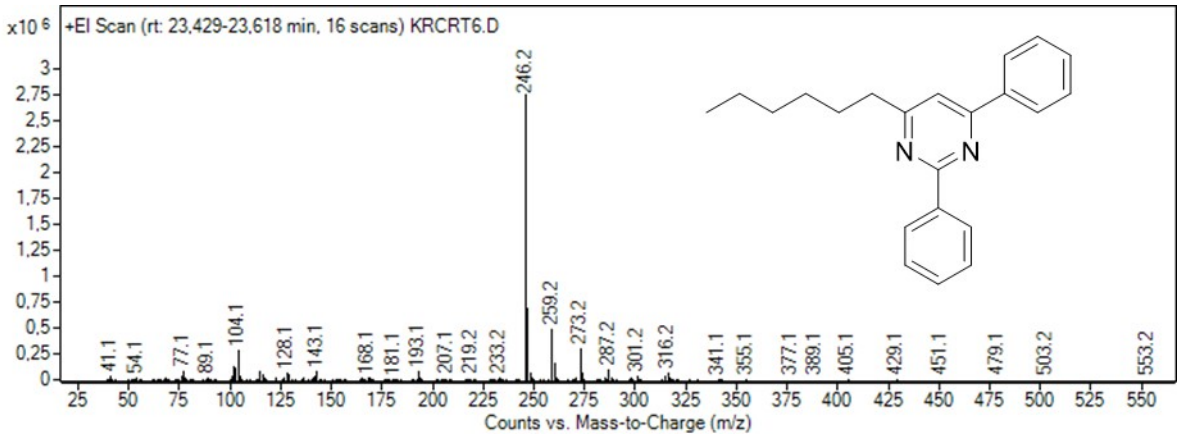

4-undecyl-2,6-diphenylpyrimidine

^{1}H NMR (400 MHz, CDCl3): δ 8.65 (d, J = 5.2 Hz, 1H), 8.49–8.41 (m, 2H), 7.49–7.45 (m, 3H), 7.02 (d, J = 5.2 Hz, 1H), 2.80 (t, J = 8.0 Hz, 2H), 1.83–1.75 (m, 2H), 1.40–1.25 (m, 14H), 0.88 (t, J = 6.8 Hz, 3H).

^{13}C NMR (101 MHz, $CDCl_3$): δ 171.1, 164.3, 156.8, 138.0, 130.4, 128.5, 128.2, 118.0, 38.0, 31.9, 29.7, 29.6, 29.5, 29.4, 29.3, 28.7, 22.7, 14.1.

MS (EI, 70 eV) m/z: 387.3 ($M^{+\cdot}$), 372.3, 355.1, 341.1, 327.0, 316.2, 302.2, 288.2, 281.1, 260.2, 253.0, 247.2, 207.1, 104.1.

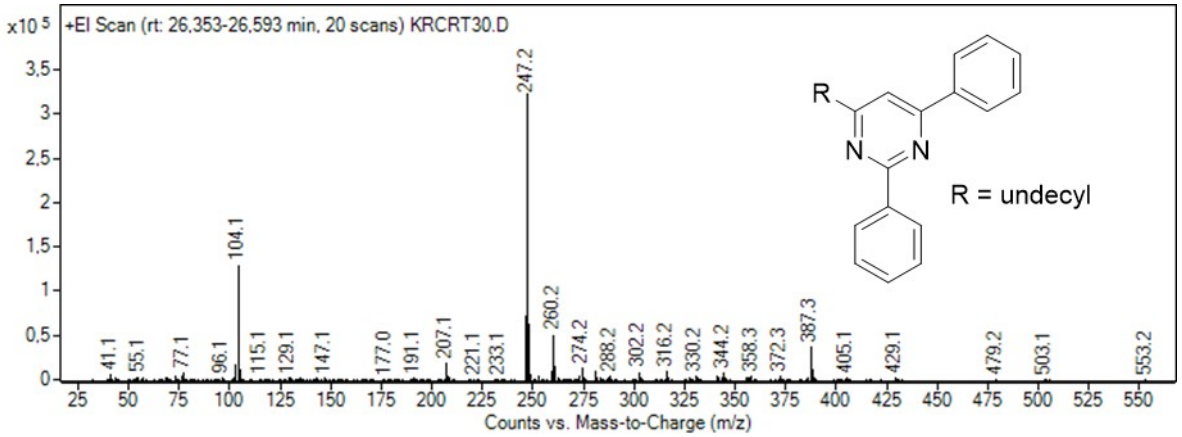

2,4-diphenyl-6,7-dihydro-5H-cyclopenta[d]pyrimidine

^{1}H NMR (400 MHz, $CDCl_3$): δ 8.45 (s, 1H), 8.40–8.34 (m, 2H), 7.48–7.38 (m, 3H), 2.94 (t, J = 6.4 Hz, 2H), 2.76 (t, J = 6.4 Hz, 2H), 1.94–1.85 (m, 4H).

^{13}C NMR (101 MHz, $CDCl_3$): δ 166.2, 162.1 157.1, 138.1, 130.0, 128.5, 127.9, 125.9, 32.2, 25.5, 22.4, 22.3.

MS (EI, 70 eV) m/z: 273.2, 272.2 ($M^{+\cdot}$), 271.2, 104.1, 65.1.

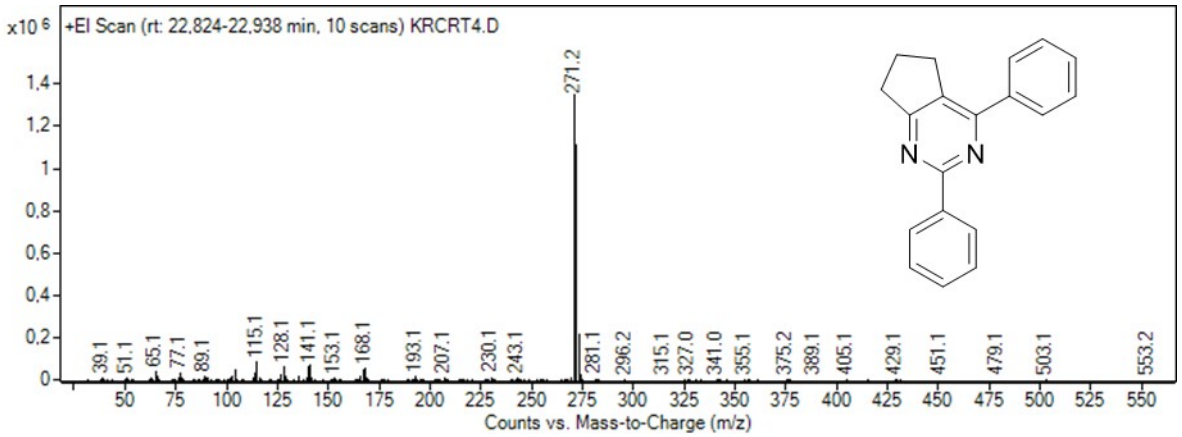

2,4-diphenyl-5,6,7,8-tetrahydroquinazoline

^{1}H NMR (500 MHz, $CDCl_3$, TMS): δ 8.5 (d, 2H), 7.7 (d, 2H), 7.5 (m, 6H), 3.1 (2H), 2,7 (d, 2H), 2.0 (m, 2H), 1.8 (m, 2H)

^{13}C NMR (125 MHz, $CDCl_3$, TMS): δ 166.7, 165.1, 161.4, 138.7, 138.1, 130.0, 129.0, 128.9, 128.3, 128.2, 128.0, 125.4, 32.7, 26.9, 22.9, 22.4.

MS (EI, 70 eV) m/z: 287.2, 286.2 ($M^{+\cdot}$), 285.2, 271.2, 258.2, 104.1.

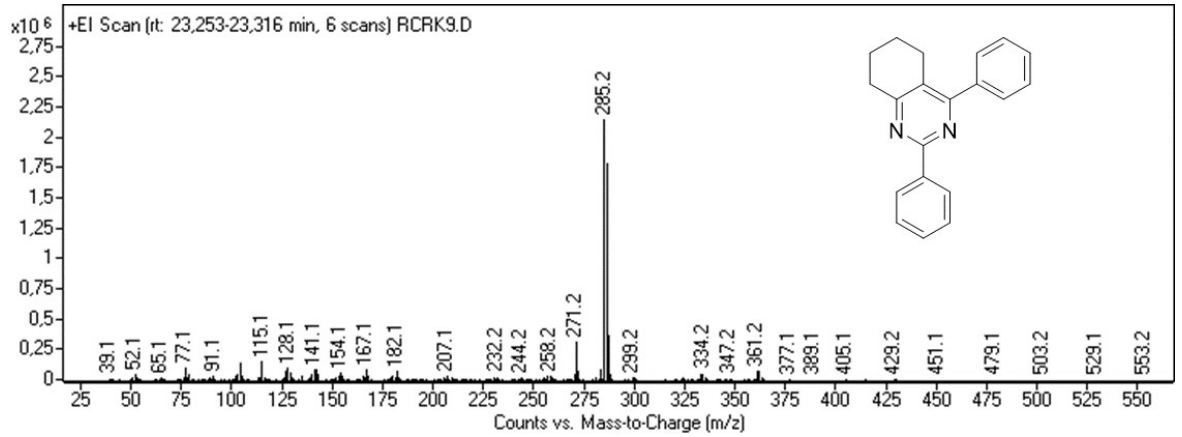

5-methyl-2,4,6-triphenylpyrimidine

^{1}H NMR (500 MHz, $CDCl_3$, TMS): δ 8.56 (d, 2H), 7.74 (m, 4H), 7.50 (m, 9H), 2.39 (s, 3H)**.**

^{13}C NMR (125 MHz, $CDCl_3$, TMS): δ 166.9, 161.4, 139.2, 137.8, 130.2, 129.3, 129.0, 128.3, 128.2, 128,1, 123.1, 77.3, 77.0, 76.7.

MS (EI, 70 eV) m/z: 323.2, 322.2 ($M^{+\cdot}$), 321.2, 217.1, 191.1, 161.1, 140.1, 115.1, 104.1, 77.1.

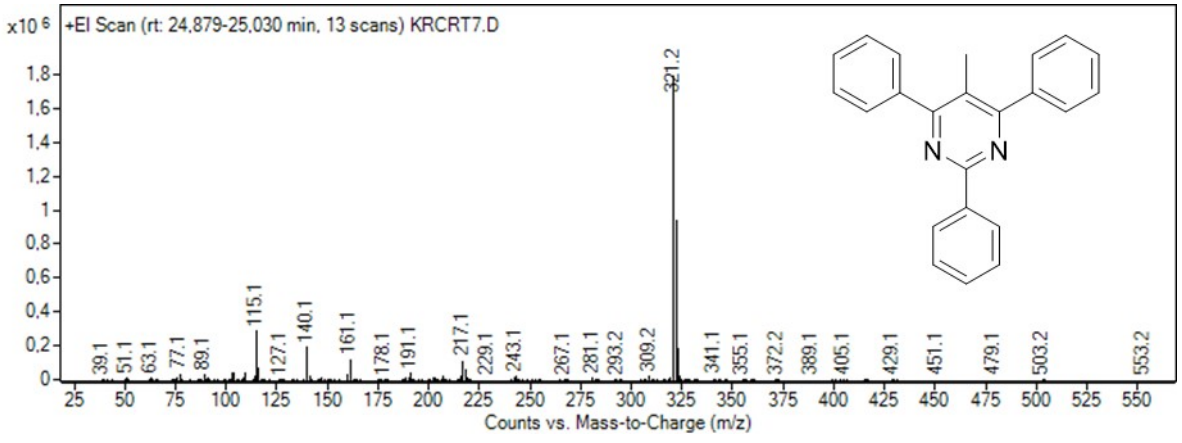

4-(4-methoxyphenyl)-2,6-diphenylpyrimidine

^{1}H NMR (500 MHz, $CDCl_3$, TMS): δ 8.72 (d, *J* = 7.3 Hz, 2H), 8.29 (d, *J* = 7.9 Hz, 4H), 7.96 (s, 1H), 7.65-7.50 (m, 6H), 7.08 (d, 2H), 3.91 (s, 3H).

^{13}C NMR (125 MHz, $CDCl_3$): δ 164.91, 164.78, 164.64, 162.34, 138.14, 131.27, 131.03, 130.92, 130.40, 129.27, 129.20, 128.85, 128.81, 127.66, 114.67, 109.81, 56.04.

MS (EI, 70 eV) m/z: 340.2, 339.2, 338.2 ($M^{+\cdot}$), 323.2, 307.2, 295.2, 235.1, 220.1, 204.1, 204.1, 193.1, 165.1, 132.1, 117.6, 102.1, 89.1, 77.1

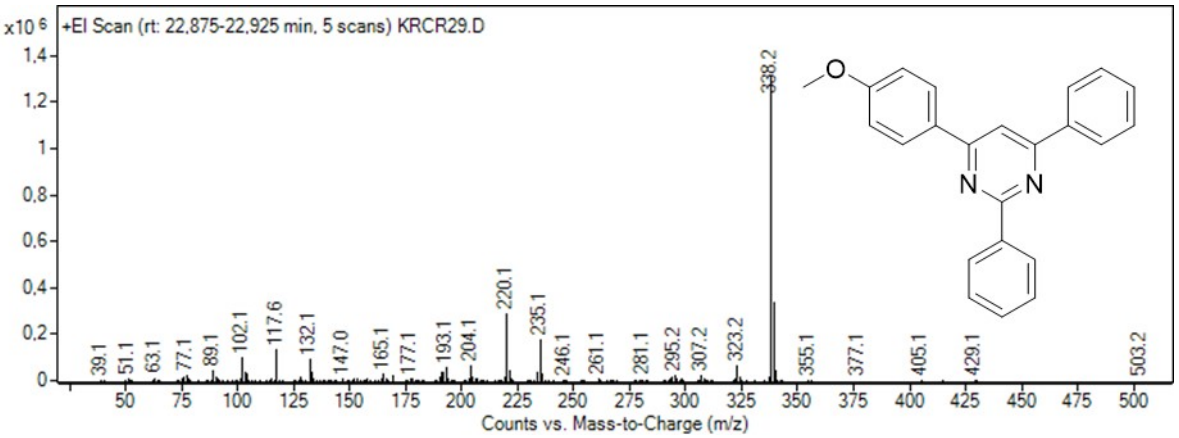

2,4-diphenyl-6-(phenylmethyl)pyrimidine

^{1}H NMR (500 MHz, $CDCl_3$, TMS): δ 8.60-8.67 (m, 2H), 8.16 (dd, *J* = 6.75 Hz, 2H), 7.57-7.48 (m, 6H), 7.38-7.30 (m, 6H), 4.25 (s, 2H).

^{13}C NMR (125 MHz, $CDCl_3$, TMS): δ 170.2, 164.5, 138.2, 137.5, 130.9, 130.8, 129.6, 129.0, 128.9, 128.7, 127.5, 127.5, 127.0, 113.8, 44.7;

MS (EI, 70 eV) m/z: 323.2, 322.2 ($M^{+\cdot}$), 321.2, 245.1, 218.1, 207.1, 191.1, 161.1, 128.1, 115.1, 104.1, 77.1.

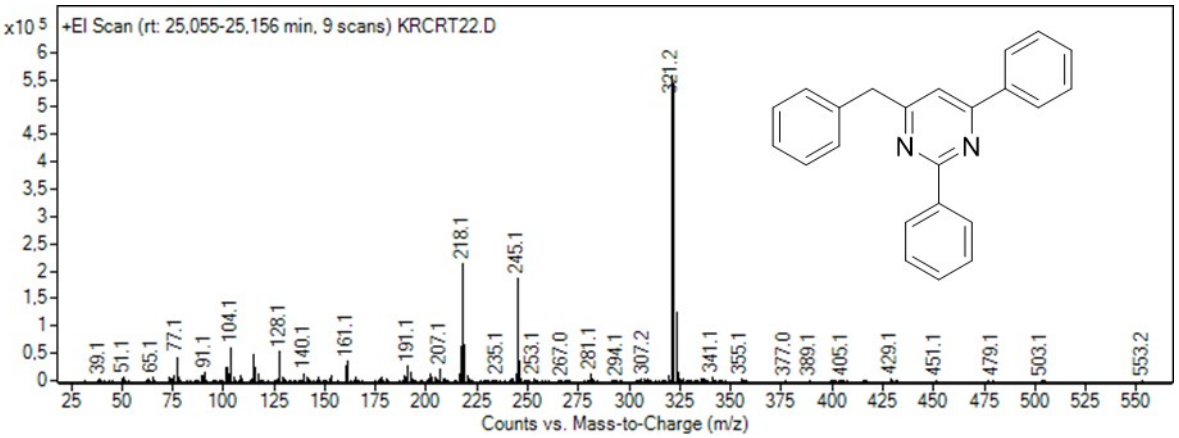

4-(3,4-dimethoxyphenyl)-2,6-diphenylpyrimidine

^{1}H NMR (500 MHz, $CDCl_3$, TMS): δ 8.71 (d, *J* = 6.0 Hz, 2H), 8.23 (d, 2H), 7.87 (s, 2H), 7.73 (d, *J* = 8.38 Hz, 1H), 7.5 (m, 6H), 6.88 (d, *J* = 8.38 Hz, 1H), 3.95 (s, 3H), 3.83 (s, 3H).

^{13}C NMR (125 MHz, $CDCl_3$, TMS): δ 164.5, 164.3, 164.2, 151.5, 149.3, 138.2, 137.6, 130.7, 130.6, 130.2, 128.9, 128.5, 128.4, 127.3, 120.3, 110.9, 110.0, 109.7, 56.1, 56.0.

MS (EI, 70 eV) m/z: 370.2, 369.2, 368.2 ($M^{+\cdot}$), 353.2, 337.2, 322.2, 308.2, 281.1, 253.1, 207.1, 184.1, 128.1, 104.1, 76.1.

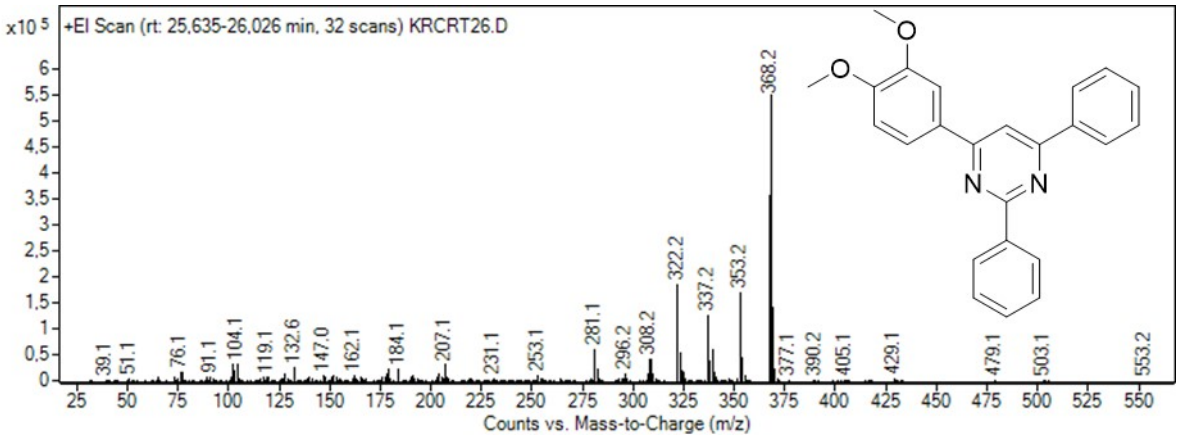

4,6-diphenyl-2-(p-tolyl)pyrimidine

^{1}H NMR (500 MHz, $CDCl_3$, TMS): δ 8.55 (d, *J* = 6.7 Hz, 2H), 8.21 (d, *J* = 7.8 Hz, 4H), 7.90 (s, 1H), 7.55-7.42 (m, 6H), 7.32 (d, *J* = 8.28 Hz, 2H), 2.38 (s, 3H).

^{13}C NMR (125 MHz, $CDCl_3$): δ 164.8, 164.7, 140.9, 137.6, 130.8, 129.3, 129.0, 128.6, 127.9, 127.4, 110.0, 21.7.

MS (EI, 70 eV) m/z: 323.2, 322.2 ($M^{+\cdot}$), 321.2, 205.1, 161.1, 128.1, 118.1, 102.1, 77.1.

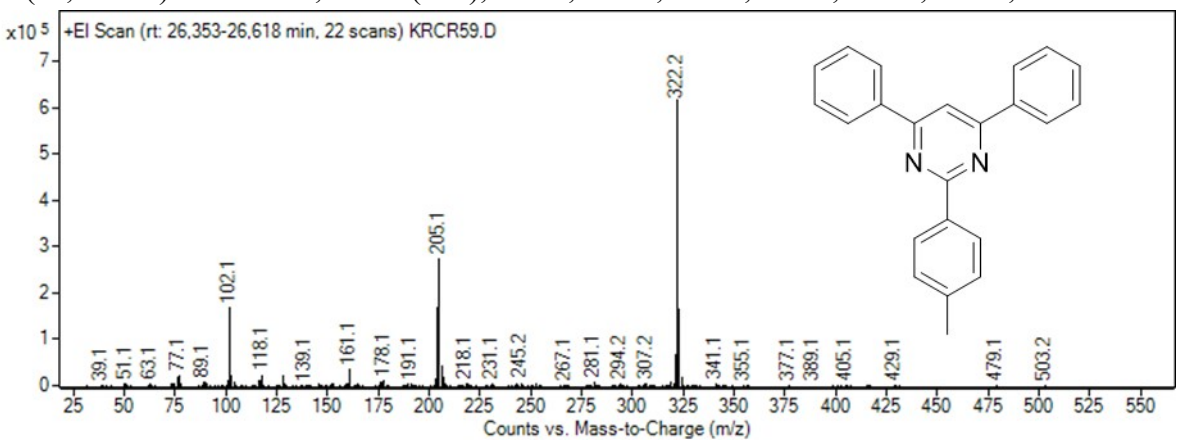

2-(4-chlorophenyl)-4,6-diphenylpyrimidine

^{1}H NMR (500 MHz, $CDCl_3$, TMS) δ 8.65 (d, J = 8.2 Hz, 2H), 8.25 (d, J = 9.6 Hz, 4H), 7.99 (s, 1H), 7.58-7.53 (m, 6H), 7.48 (d, J = 7.56 Hz, 2H).

^{13}C NMR (125 MHz, $CDCl_3$ TMS): δ 164.8, 163.4, 137.3, 136.7, 136.6, 130.8, 129.8, 128.9, 128.6, 127.2, 110.4.

MS (EI, 70 eV) m/z: 346.1, 345.1, 344.1, 343.1 ($M^{+\cdot}$), 281.1, 207.1, 137.0, 103.1, 76.1.

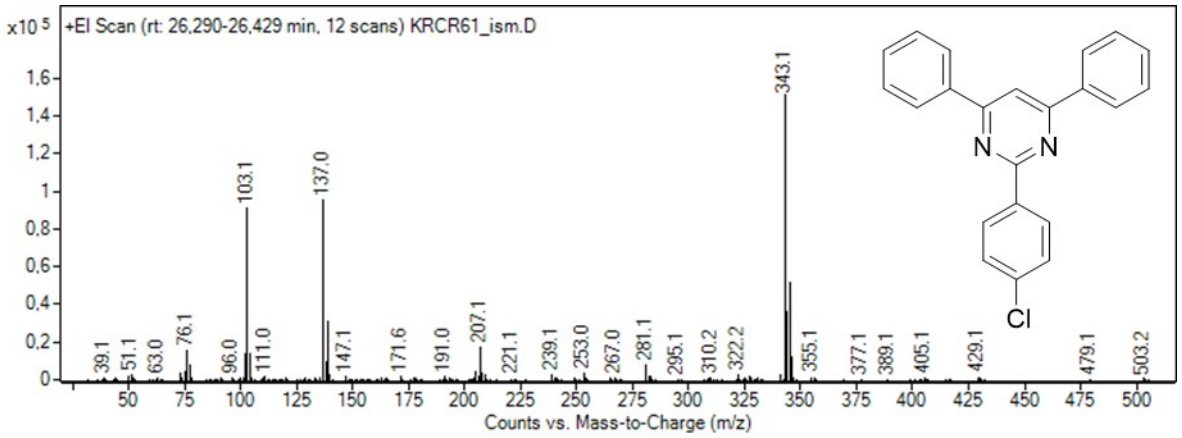

4-(4,6-diphenylpyrimidin-2-yl)aniline

^{1}H NMR (500 MHz, DMSO-d6, TMS): δ 8.43 (d, *J* = 7.3 Hz, 2H), 8.36 (m, 4H), 8.31 (s, 1H), 6.68-6.74 (m, 2H), 5.64 (br, 2H).

^{13}C NMR (125 MHz, DMSO-d6, TMS): δ 163.8, 163.4, 151.3, 136.9, 130.5, 129.2, 128.5, 126.9, 124.5, 113.0, 108.1.

MS (EI, 70 eV) m/z: 324.2, 323.2 ($M^{+\cdot}$), 322.2, 204.1, 161.6, 128.1, 118.1, 102.1, 91.1, 77.1.

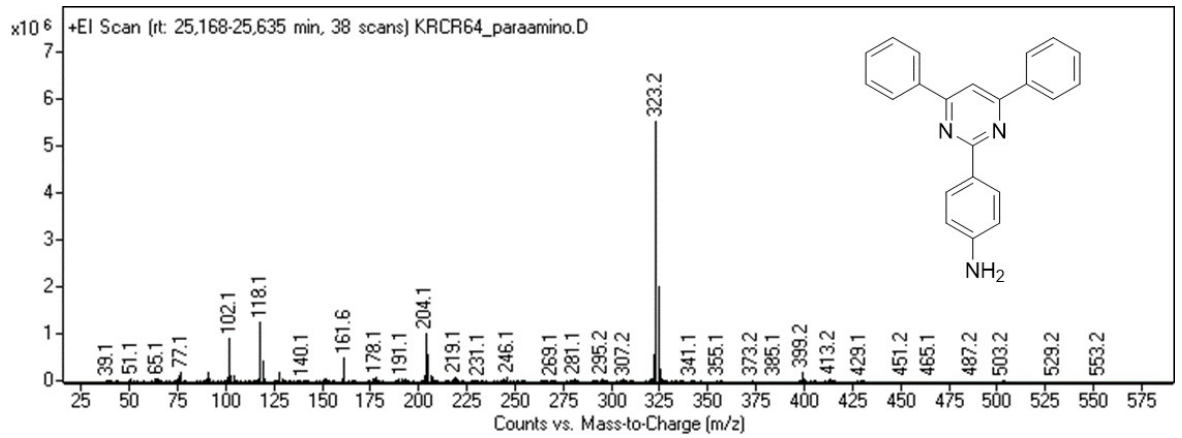

*2-(4-methoxyphenyl)-4,6-diphenylpyrimidine (**4n**)*

^{1}H NMR (500 MHz, $CDCl_3$, TMS): δ 8.71 (d, *J* = 8.4 Hz, 2H), 8.29 (d, *J* = 7.1 Hz, 4H), 7.95 (s, 1H), 7.56 (m, 6H), 7.07 (d, *J* = 8.4 Hz, 2H), 3.91 (s, 3H).

^{13}C NMR (125 MHz, $CDCl_3$): δ 164.7, 164.3, 161.9, 137.8, 130.7, 130.2, 128.9, 127.3, 113.8, 109.6, 55.6.

MS (EI, 70 eV) m/z: 338.2 ($M^{+\cdot}$), 323.2, 295.1, 204.1, 169.1, 133.1, 102.1, 77.1.

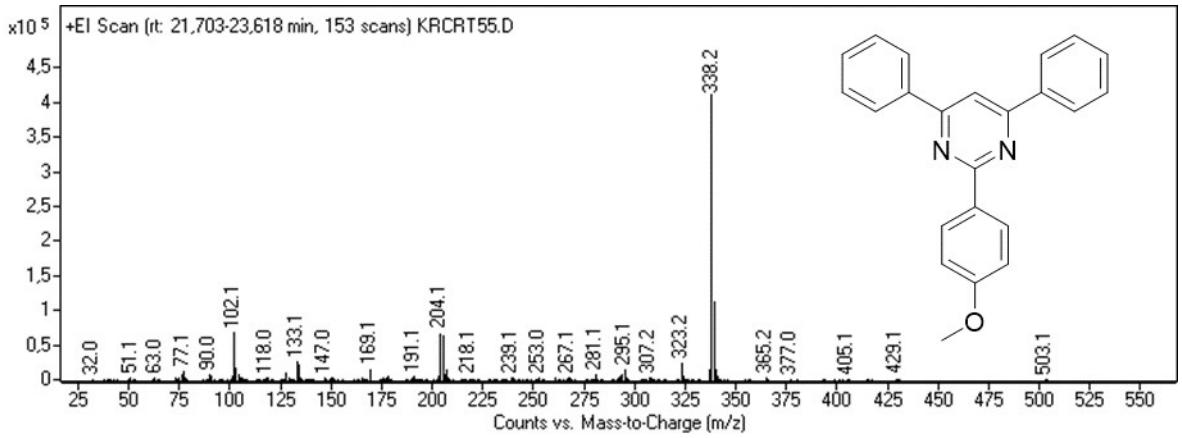
x10 5
+EI Scan (rt: 21,703-23,618 min, 153 scans) KRCRT55.D
4,5
4
3,5
3
2,5
2
1,5
1
0,5
0
338.2
102.1
204.1
32.0
51.1
63.0
77.1
90.0
118.0
133.1
147.0
169.1
191.1
218.1
239.1
253.0
267.1
281.1
295.1
307.2
323.2
365.2
377.0
405.1
429.1
503.1
25 50 75 100 125 150 175 200 225 250 275 300 325 350 375 400 425 450 475 500 525 550
Counts vs. Mass-to-Charge (m/z)
N
N
O

REFERENCES

1 A. A. Ádám, S. B. Nagy, Á. Kukovecz, Z. Kónya, P. Sipos and G. Varga, *Chem. Commun.*, 2024, 10520–10523.

2 X. Du, G. Zou, Y. Zhang and X. Wang, *J. Mater. Chem. A*, 2013, **1**, 8411–8416.

3 J. Yu, J. Sunarso, Y. Zhu, X. Xu, R. Ran, W. Zhou and Z. Shao, *Chem. Eur. J.*, 2016, **22**, 2719–2727.

4 B. K. Slinker, *J. Mol. Cell. Cardiol.*, 1998, **30**, 723–731.

5 S. Sultana Poly, S. M. A. H. Siddiki, A. S. Touchy, K. W. Ting, T. Toyao, Z. Maeno, Y. Kanda and K. I. Shimizu, *ACS Catal.*, 2018, **8**, 11330–11341.

6 C. Savarimuthu Selvan, R. Rengan and J. G. Malecki, *J. Org. Chem.*, 2024, **89**, 11148–11160.

7 N. Deibl and R. Kempe, *Angew. Chem. Int. Ed.*, 2017, **56**, 1663–1666.

8 N. Deibl, K. Ament and R. Kempe, *J. Am. Chem. Soc.*, 2015, **137**, 12804–12807.

9 M. Mastalir, M. Glatz, E. Pittenauer, G. Allmaier and K. Kirchner, *Org. Lett.*, 2019, **21**, 1116–1120.

10 M. Mastalir, M. Glatz, E. Pittenauer, G. Allmaier and K. Kirchner, *J. Am. Chem. Soc.*, 2016, **138**, 15543–15546.

11 K. Van Aken, L. Strekowski and L. Patiny, *Beilstein J. Org. Chem.*, 2006, **2**, 1–7.